

DIFFRACTION PHYSICS OVERVIEW

Uri Maor

Raymond and Beverly Sackler Faculty of Exact Science

Tel Aviv University, Tel Aviv, 69978, Israel

Standard Model and LHC

Niels Bohr International Academy And Discovery

Center

Copenhagen 10-13 April, 2012

INTRODUCTION

- **Hard pQCD deals with short distance strong interactions of high transverse momentum partons.**
- **Soft QCD is associated with low transverse momentum partons, separated by large distances, where we cannot utilize perturbative methods. npQCD calculations are based on phenomenological models, foremost (but not only) the Regge pole model with a leading Pomeron (P) term.**
- **Total and elastic (but NOT diffractive) cross sections in the ISR-Tevatron range are well reproduced by the DL model, where**

$$\alpha_P(t) = 1 + \Delta_P + \alpha'_P t \quad \Delta_P = 0.08, \alpha'_P = 0.25 \text{GeV}^{-2}.$$

- **Given a super critical P ($\Delta_P > 0$), σ_{el} grows indefinitely faster than σ_{tot} and will, eventually, get larger! This paradox is resolved in models where s-channel unitarity screening is enforced on $a_{el}(s, b)$.**

The physics, just presented, is deficient in a few fundamental issues:

- Soft diffractive channels are analogous to the elastic channel. Indeed, Good-Walker (GW) have observed that in p-p scattering the eigen states of the scattering matrix are linear combination of the proton and diffractive states.
- t-channel unitarity dynamics initiates additional screenings which should be taken into account. This is formalized in updated \mathbb{P} models through multi- \mathbb{P} t-channel interactions.
- Gribov's partonic interpretation of the soft \mathbb{P} enables a re-examination of soft versus hard Pomerons.

Most of this talk will center on updated \mathbb{P} models which unify the soft elastic and diffractive physics. I shall briefly refer to other models based on partonic concepts. I shall not discuss simulations and parametrizations.

S-CHANNEL UNITARITY

Enforcing s-channel unitarity is model dependent.

Assume a single dimension unitarity equation, $2\text{Im}a_{el}(s, b) = |a_{el}(s, b)|^2 + G^{in}(s, b)$.

This is no more than a statement that $\sigma_{tot}(s, b) = \sigma_{el}(s, b) + \sigma_{inel}(s, b)$.

Its general solution can be written as

$$a_{el}(s, b) = i \left(1 - e^{-\Omega(s, b)/2}\right) \quad \text{and} \quad G^{in}(s, b) = 1 - e^{-\Omega(s, b)},$$

where $\Omega(s, b)$ is arbitrary. It induces a unitarity bound of $|a_{el}(s, b)| \leq 2$.

In a **Glauber type** eikonal approximation the input opacity $\Omega(s, b)$ is real,

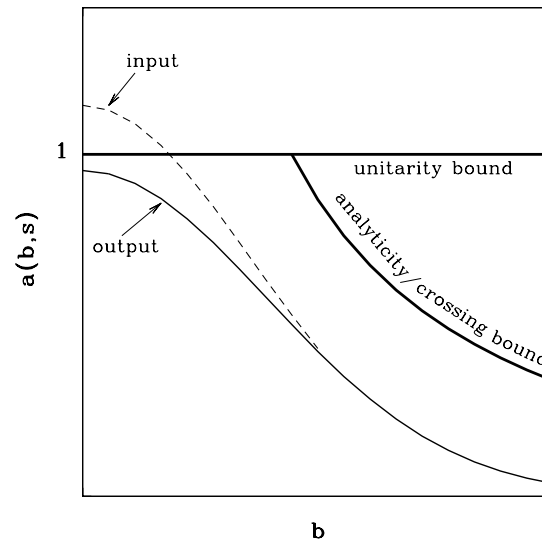
i.e. $a_{el}(s, b)$ is imaginary. It equals the imaginary part of the input Born term,

a single IP exchange in our context. The output bound is $|a_{el}(s, b)| \leq 1$, which

is the black disc bound. An added bonus is that the eikonal model reproduces

the s and t dependence of the diffractive dip (shoulder) observed in p(\bar{p})-p

elastic scattering. **The real part is obtained from dispersion relations.**



The figure shows the effect of eikonal s-channel screening, securing that the screened elastic amplitude is bounded by unity. The figure illustrates, also, the R_{el} bound implied by analyticity/crossing symmetry.

The total, elastic and inelastic cross sections are given by

$$\sigma_{tot} = 2 \int d^2b \left(1 - e^{-\Omega(s,b)/2} \right),$$

$$\sigma_{el} = \int d^2b \left(1 - e^{-\Omega(s,b)/2} \right)^2,$$

$$\sigma_{inel} = \sigma_{tot} - \sigma_{el} = \int d^2b \left(1 - e^{-\Omega(s,b)} \right).$$

GOOD-WALKER DECOMPOSITION

Consider a system of two orthonormal states, a hadron Ψ_h and a diffractive state Ψ_D . Ψ_D replaces the continuous population of the diffractive Fock states.

It has a non specified mass. The GW mechanism stems from the observation that these states do not diagonalize the 2x2 interaction matrix \mathbf{T} .

Assume that Ψ_1 and Ψ_2 are eigen states of \mathbf{T} . We get,

$$\Psi_h = \alpha \Psi_1 + \beta \Psi_2, \quad \Psi_D = -\beta \Psi_1 + \alpha \Psi_2, \quad \alpha^2 + \beta^2 = 1,$$

with 4 elastic GW amplitudes ($i,k=1,2$), $A_{i,k}^{i',k'} = \langle \Psi_i \Psi_k | \mathbf{T} | \Psi_{i'} \Psi_{k'} \rangle = A_{i,k} \delta_{i,i'} \delta_{k,k'}$.

For initial $p(\bar{p}) - p$ we have $A_{1,2} = A_{2,1}$. The elastic, SD and DD amplitudes are:

$$\begin{aligned} a_{el}(s, b) &= i\{\alpha^4 A_{1,1} + 2\alpha^2 \beta^2 A_{1,2} + \beta^4 A_{2,2}\}, \\ a_{sd}(s, b) &= i\alpha\beta\{-\alpha^2 A_{1,1} + (\alpha^2 - \beta^2)A_{1,2} + \beta^2 A_{2,2}\}, \\ a_{dd} &= i\alpha^2 \beta^2\{A_{1,1} - 2A_{1,2} + A_{2,2}\}. \end{aligned}$$

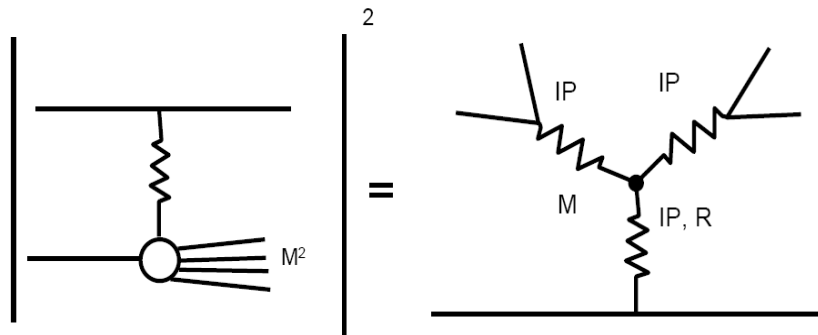
The eikonal re-scatterings of the incoming projectiles are summed over the GW eigen states.

Updated \mathcal{P} eikonal models are two channel in which:

$$\Omega_{i,k}(s, b) = \nu_{i,k}(s) \Gamma_{i,k}(s, b) \quad \text{and} \quad \nu_{i,k}(s) = g_i g_k \left(\frac{s}{s_0}\right)^{\Delta \mathcal{P}}.$$

The b-profile $\Gamma_{i,k}(s, b)$ is parametrized so as to reproduce the elastic and diffractive channels $\frac{d\sigma}{dt}$ in the forward cone.

The profile is parametrized differently in each \mathcal{P} models. However, all the corresponding numerics are compatible in the forward t-cone.



MULTI POMERON INTERACTIONS

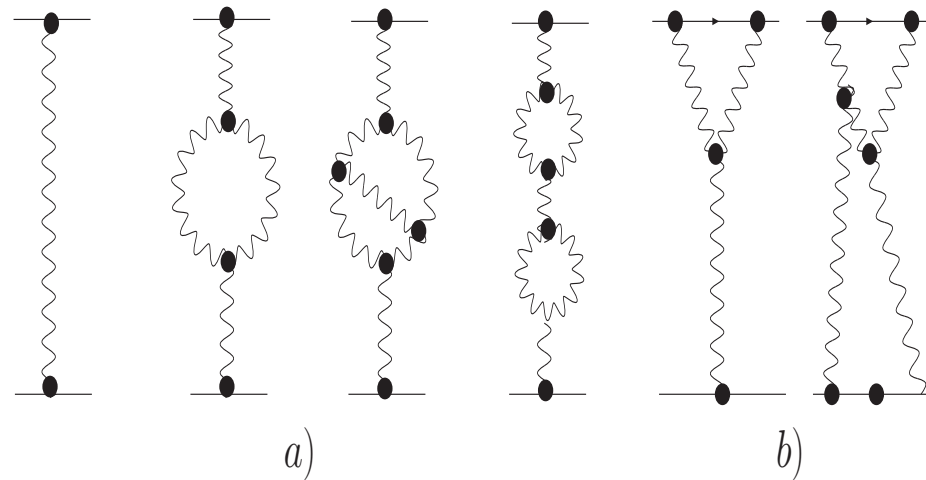
Mueller(1971) applied 3 body unitarity to equate the cross section of $a + b \rightarrow M + b$ to the triple Regge diagram $a + b + \bar{b} \rightarrow a + b + \bar{b}$.

The signature of this presentation is a triple vertex with a leading $3P$ term.

The corresponding cross section is

$$M^2 \frac{d\sigma^{3P}}{dt dM^2} = \frac{g_p^2(t)g_p(0)G_{3P}}{16 \pi^2} \left(\frac{s}{M^2}\right)^{2\alpha_P(t)-2} \left(\frac{M^2}{s_0}\right)^{\alpha_P(0)-1}, \quad \frac{m_p^2}{M^2} \ll 1 \text{ and } \frac{M^2}{s} \ll 1.$$

The leading energy/mass dependences are $\frac{d\sigma^{3P}(t=0)}{dt dM^2} \propto s^{2\Delta_P} \left(\frac{1}{M^2}\right)^{1+\Delta_P}$.



Mueller's $3\mathbb{P}$ approximation for "high mass" SD is the lowest order of a large sequence of multi Pomeron interactions not included in the GW mechanism. This feature is compatible with t-channel unitarity. The figure shows the low order \mathbb{P} Green's function.

- a) Enhanced diagrams which renormalize (in low order) the \mathbb{P} propagator.
 - b) Semi-enhanced diagrams which renormalize (in low order) the \mathbb{P} -p vertexes.
- The diagrams complexity leads to model dependent summing algorithms.

The analysis of soft diffraction is complicated due to the lack of uniform experimental and theoretical definitions of its signatures and mass bounds.

Note that: The upper bound on the "low mass" is not defined. Kaidalov, at the time, bounded the "low mass" diffraction from above by the lower bound of the "high mass" diffraction. i.e. in his parametrization there is no overlap between "low mass" and "high mass" diffraction. This is practiced also by KMR, Ostapchenko and Kaidalov-Poghosyan (KP).

In GLM, GW and non GW diffraction have the same upper bound $\frac{M^2}{s} \leq 0.05$.

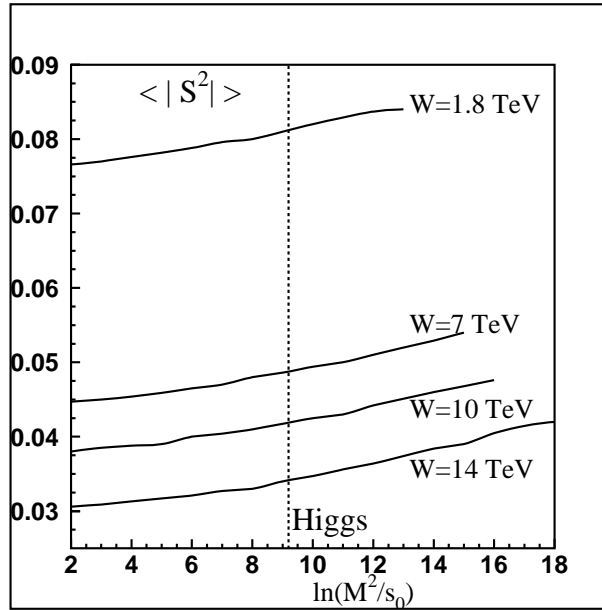
Consequently, GLM diffraction is predominantly GW. The diffraction of Kaidalov, KMR, Ostapchenko and KP is predominantly non GW.

At LHC energies the difference between the two definitions becomes significant.

LRG SURVIVAL PROBABILITY

The experimental signature of a \mathbb{P} exchanged reaction is a large rapidity gap (LRG), devoid of hadrons in the $\eta - \phi$ lego plot, $\eta = -\ln(\tan\frac{\theta}{2})$.

S^2 , the LRG survival probability, is a unitarity induced suppression factor of non GW diffraction, soft or hard: $S^2 = \sigma_{diff}^{scr} / \sigma_{diff}^{nscr}$. It is the probability that the LRG signature will not be filled by debris (partons and/or hadrons) originating from either the s-channel re-scatterings of the spectator partons, or by the t-channel multi \mathbb{P} interactions. Denote the gap survival factor initiated by s-channel eikonalization S_{eik}^2 , and the one initiated by t-channel multi \mathbb{P} interactions S_{enh}^2 . S^2 is obtained from an integral convolution of S_{eik}^2 and S_{enh}^2 . A simpler reasonable approximation is $S^2 = S_{eik}^2 \cdot S_{enh}^2$.



Assuming no screening, $\alpha_{\mathcal{P}}$ can be obtained from either the s dependence of $\sigma_{tot}, \sigma_{el}, \sigma_{sd}$, or from σ_{sd} "high mass" distribution. s and t screenings initiate a slow decrease in the value of $\Delta_{\mathcal{P}}^{eff}$ with growing s . The screenings of $\sigma_{tot}, \sigma_{el}$ and σ_{sd} are not identical, resulting in a dependence of $\Delta_{\mathcal{P}}^{eff}$ on the channel it is obtained from. The figure above shows the dependence of S^2 on s and M^2 . Note that the M^2 dependence is considerably more moderate than the dependence on s . Hence, the value of $\Delta_{\mathcal{P}}^{eff}$ is closer to its non screened input.

THE PARTONIC POMERON

The microscopic sub structure of the Pomeron is provided in **Gribov's partonic interpretation of Regge theory**, in which the slope of the Pomeron trajectory is related to the mean transverse momentum of the partonic dipoles constructing the Pomeron, and consequently, the running QCD coupling.

$$\alpha'_{\mathbb{P}} \propto 1 / \langle p_t \rangle^2, \quad \alpha_S \propto \pi / \ln(\langle p_t^2 \rangle / \Lambda_{QCD}^2) \ll 1.$$

Intuitively, these relations suggest a connection between the soft and hard Pomerons. This is a non trivial relation as **the soft \mathbb{P} is a simple moving pole in J-plane, while, the BFKL \mathbb{P} is a branch cut**. Recall, though, that the BFKL \mathbb{P} is commonly approximated as a simple J-pole with $\Delta_{\mathbb{P}} = 0.2 - 0.3$ and $\alpha'_{\mathbb{P}} = 0$. In the Following I shall discuss $4\mathbb{P}$ models rooted in Gribov's partonic \mathbb{P} theory. The models are conceptually similar, but differ in their \mathbb{P} diagram summations.

- **GLM (Tel AVIV)** input is a single \mathbb{P} , $\Delta_{\mathbb{P}} = 0.20$, $\alpha'_{\mathbb{P}} \simeq 0$. The hardness of the exchanged \mathbb{P} depends on the unitarity screenings. In the limit of no screening the \mathbb{P} is hard, whereas, in the limit of strong screening it is soft. GLM utilize pQCD procedures, where $n\mathbb{P} \rightarrow m\mathbb{P}$ reduces to a sequence of $G_{3\mathbb{P}}$ vertexes (Fan diagrams). $G_{3\mathbb{P}}$ and $\gamma^2 = \int G_{3\mathbb{P}} d^2 p_t$ are free parameters.

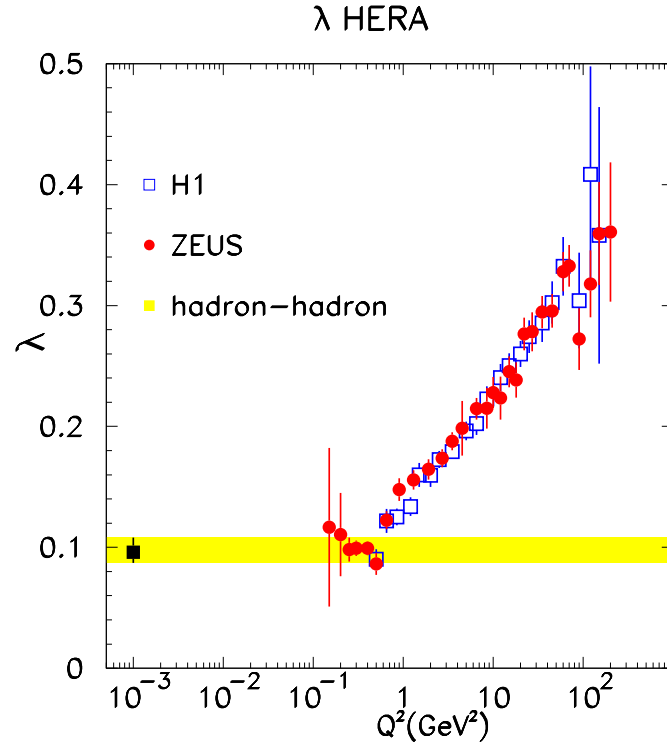
- **KMR (Durham)** input is a single \mathbb{P} , $\Delta_{\mathbb{P}} = 0.3$, $\alpha'_{\mathbb{P}} \propto 1/p_t^2$. The hardness of the exchanged \mathbb{P} depends on p_t .

KMR $n\mathbb{P} \rightarrow m\mathbb{P}$ couplings are $g_m^n = \frac{1}{2} g_N n m \lambda^{n+m-2} = \frac{1}{2} n m G_{3\mathbb{P}} \lambda^{n+m-3}$.

$n + m > 2$, $G_{3\mathbb{P}} = \lambda g_N$. λ and g_N are free parameters.

Ostapchenko and KP have a different normalization.

- **Ostapchenko (Bergen)** has 2 Pomerons, soft: $\Delta_{\mathbb{P}} = 0.17$, $\alpha'_{\mathbb{P}} = 0.11$, and hard: $\Delta_{\mathbb{P}} = 0.31$, $\alpha'_{\mathbb{P}} = 0.085$.
- **KP (Moscow, CERN)** is a single channel soft \mathbb{P} model with many secondary Regge trajectories. $\Delta_{\mathbb{P}} = 0.12$, $\alpha'_{\mathbb{P}} = 0.22$.



SOFT AND HARD POMERONS

GLM and KMR \mathbb{P} models have a single \mathbb{P} , with similar $\Delta_{\mathbb{P}}$ and $\alpha'_{\mathbb{P}}$ input values.

The obvious question is if this observation conveys a dynamical property of the \mathbb{P} , where an input hard pQCD \mathbb{P} can be softened by unitarity screening (GLM), or the decrease of its partons' transverse momentum (KMR).

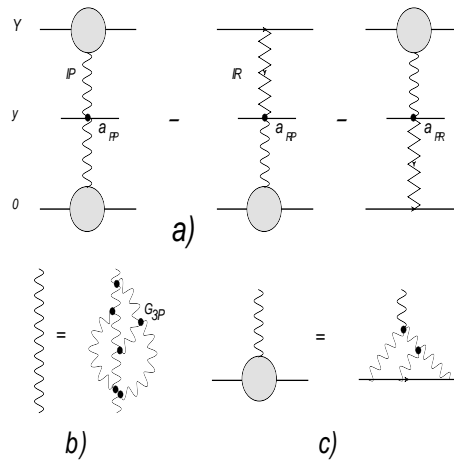
The experimental study of e-p DIS provides a "laboratory" in which we can investigate the Pomeron properties as a function of its kinematic variables. Indeed, HERA e-p DIS data is a rich source of information on \mathbb{P} features.

The figure presents $\sigma(\gamma^* + p \rightarrow p + X) \propto s^\lambda$, as a function of Q^2 . $\lambda = \Delta_{\mathbb{P}}$.

It shows the transition from the **soft (non perturbative) Pomeron** to the **hard (perturbative) Pomeron**.

As seen, at very small Q^2 , $\Delta_{\mathbb{P}} \simeq 0.1$, compatible with the hadronic soft data.

At higher Q^2 , up to $\simeq 100 \text{ GeV}^2$, $\Delta_{\mathbb{P}}$ **grows smoothly toward** $\Delta_{\mathbb{P}} \simeq 0.30 - 0.35$.

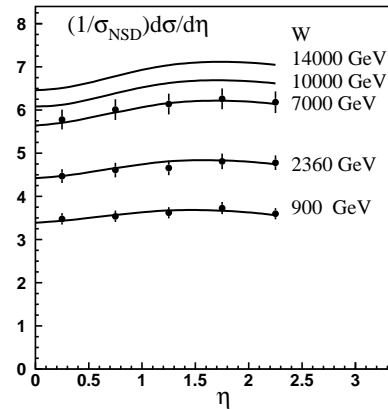


LHC CROSS SECTION DATA

A conceptual issue, which should be settled by LHC study of soft scattering data, is if the ISR-Tevatron soft data can be smoothly extrapolated to LHC.

A) NSD data on $dN_{ch}/d\eta = \{1/\sigma_{NSD}\}d\sigma/d\eta$, the charged multiplicity density distribution, has been published by ALICE, CMS and ATLAS at central pseudo rapidity $-2.5 \leq \eta \leq 2.5$. This data provides an additional perspective on the \mathbb{P} model in the framework of Gribov's \mathbb{P} calculus.

$dN_{ch}/d\eta$ is calculated using Mueller diagrams and GLM fitted parameters.



We add 3 parameters: a_{IP} , $a_{IPR} = a_{RIP}$, accounting for hadron emission from the exchanged IP or Reggeon. Q is the average p_t of the produced mini-jets.

The data base for this fit covers the 546-7000 TeV range and was taken over many years, with different approaches.

We have obtained a satisfactory fit of this data. The shown figure presents a very good GLM fit to CMS data at 900, 2360, 7000 GeV. The two sets of fitted parameters are compatible.

Our calculations reproduce the SppS-LHC inclusive data.

| ATLAS | ALICE | CMS | TOTEM |
|------------------------|------------------------|--------------------------------|----------------------------|
| $69.4 \pm 2.4 \pm 6.9$ | $72.7 \pm 1.1 \pm 5.1$ | $71.8 \pm 1.1 \pm 2.0 \pm 7.9$ | $73.5 \pm 0.6 + 1.8 - 1.3$ |

TABLE I: LHC σ_{inel} at 7 TeV

| Achilli et al. | Block-Halzen | GLM | KP | KMR |
|----------------|--------------|------|------|-----------|
| 60-75 | 69.0 | 71.3 | 70.0 | 62.6-67.1 |

TABLE II: σ_{inel} model predictions at 7 TeV

B) $\sigma_{inel} = \sigma_{tot} - \sigma_{el} = \sigma_{sd} + \sigma_{dd} + \sigma_{nd}$. The early LHC measurements of σ_{inel} were derived from the minimum bias data samples. TOTEM is the only collaboration which obtains σ_{inel} as a cross sections difference. The 2 tables compare the 7 TeV σ_{inel} data and its model predictions. **The LHC average $\langle \sigma_{inel} \rangle = 71.1 \text{mb}$, is well reproduced by GLM.**

C) TOTEM recent results at 7 TeV, $\sigma_{tot} = 98.3 \pm 2.71 \text{mb}$, $\sigma_{el} = 24.8 \pm 2.81 \text{mb}$.

| | Achilli et al. | Block-Halzen | Halzen-Igi et al. | GLM | KP | KMR |
|--------------------------|----------------|--------------|-------------------|------|------|------|
| $\sigma_{tot} \text{mb}$ | 91.6 | 95.4 | 96.1 | 94.2 | 96.4 | 89.0 |
| $\sigma_{el} \text{mb}$ | | 26.4 | | 22.9 | 24.8 | 21.9 |

TABLE III: σ_{tot} and σ_{el} theoretical predictions.

The table presents the theoretical predictions.

The theoretical predictions are moderately below the TOTEM cross sections.

\mathbb{P} models' problem is that their formalism has a large number of free parameters, in no proportion to their small adjusted data base.

In my opinion, prior to theoretical modifications, one should improve the adjustment procedures.

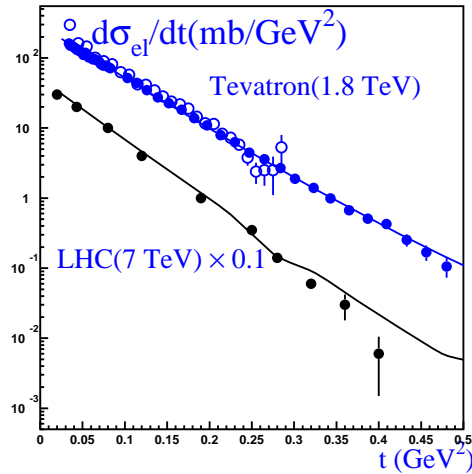
The predictions of Halzen et al. are some what better than the competition.

However, this class of partonic models has two deficiencies:

- i) It is strictly a phenomenological parton model based on parametrizations.
- ii) It does not incorporate diffraction with elastic scattering.

D) GLM and KMR reproduce TOTEM's $d\sigma_{el}(t \leq 0.5 GeV^2)/dt$, see GLM figure.

So does a recent DL model based on soft+hard \mathbb{P} . TOTEM forward elastic slope is $B_{el} = 20.1 \pm 0.36 GeV^{-2}$. GLM get a very close value $B_{el} = 19.8 GeV^{-2}$.



As it stands, none of the existing models reproduces TOTEM's $\frac{d\sigma_{el}}{dt}$ at high $t > 0.5 GeV^2$, in particular the position and the shape of the p-p diffraction dip.

E) LHC diffractive data is limited, at this stage. ALICE has measured

$\sigma_{sd} = 14.16 \pm 3mb$, and $\sigma_{dd} = 8.86 \pm 3mb$, where $M \leq 200GeV$, ($\xi \leq 0.0008$).

GLM values for "low mass" diffraction at 7 TeV are lower, $\sigma_{sd} = 10.5mb$

and $\sigma_{dd} = 6mb$. ATLAS preliminary SD cross section at 7 TeV is $\sigma_{sd} = 17 - 21mb$

for $M > 15.7GeV$, ($\xi > 6.6 \times 10^{-7}$).

EXCEEDINGLY HIGH ENERGY BEHAVIOR

Saturating the s-unitarity and analyticity/crossing bounds we get the **Froissart-Martin bound**,

$$\sigma_{tot} \leq C \log^2(s/s_0), \text{ in which } C = \pi/2m_\pi^2.$$

The coefficient C is far too large to make this bound useful.

Note that, The Froissart-Martin $\log^2 s$ behavior relates to the bound, NOT to the total cross section which can grow more rapidly than $\log^2 s$ as long as it is below the bound.

Hence, a σ_{tot} model with $\log^2 s$ behavior is compatible with, but NOT induced, by Froissart-Martin bound!

In a single channel non GW model, $\sigma_{el} \leq \frac{1}{2}\sigma_{tot}$ **and** $\sigma_{inel} \geq \frac{1}{2}\sigma_{tot}$. Equality is reached at the saturated black disc bound, where $\sigma_{el} = \sigma_{inel} = \frac{1}{2}\sigma_{tot}$.

Single channel models neglect the GW mixing of the proton and "low mass" diffractive wave functions. In GW multi-channel models we distinguish between

GW and non GW diffraction.

In such a model, we obtain the **Pumplin bound**: $(\sigma_{el} + \sigma_{diff}^{GW}) \leq \frac{1}{2}\sigma_{tot}$.

Equality is attained at the black disc saturation. The implication is that in a

multi-channel GW model, $\sigma_{el} \leq \frac{1}{2}\sigma_{tot} - \sigma_{diff}^{GW}$, $\sigma_{inel} \geq \frac{1}{2}\sigma_{tot} + \sigma_{diff}^{GW}$.

Recently, Block and Halzen analyzed an AUGER event at $W = 57 \pm 6 TeV$.

They get: $\sigma_{tot} = 134.8mb$ and $\sigma_{inel} = 90mb$, $\frac{\sigma_{inel}}{\sigma_{tot}} = 0.67$.

The corresponding GLM predictions are:

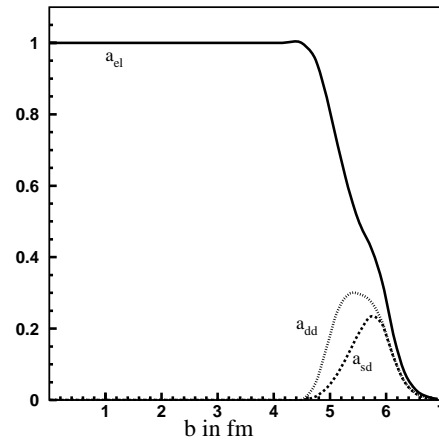
$\sigma_{tot} = 122mb$, $\sigma_{el} = 31.1mb$, $\sigma_{inel} = 90.9$, $\sigma_{sd} = 21mb$, $\sigma_{dd} = 13.5mb$, $\frac{\sigma_{inel}}{\sigma_{tot}} = 0.75$.

The implication from those very different models is that s-channel saturation will be attained, if at all, at energies of the order of the Planck scale. The

basic GW amplitudes are $A_{1,1}$, $A_{1,2}$ and $A_{2,2}$. with which we construct a_{el} , a_{sd} and a_{dd} . The $A_{i,k}$ amplitudes are bounded by the unitarity black disc bound

of unity. $a_{el}(s, b)$ reaches this bound. at a given (s, b) , when, and only when

$A_{1,1}(s, b) = A_{1,2}(s, b) = A_{2,2}(s, b) = 1$, independent of the GW mixing parameter.



When $a_{el}(s, b) = 1$, $a_{sd}(s, b) = a_{dd}(s, b) = 0$.

Lets re-check the diffractive channels at exceedingly high energies. The elastic amplitude which is essentially black, has a high b tail where $a_{el}(s, b) < 1$. In this domain diffraction can survive. The Figure shows the GLM elastic, SD and DD amplitudes at the Planck scale. Note that the analyticity/crossing R_{el} bound is not effective even at the Planck scale.